

Theory of Hypernuclei

W.M. Alberico

Dip. di Fisica Teorica and INFN, Torino, Italy

STRANGENESS, SPIN and QGP

European Graduate School “Complex Systems of Hadrons and Nuclei”

(Copenhagen, Giessen, Helsinki, Jyväskylä, Torino)

Villa Gualino, Torino, 9-15 October, 2005

Lecture II

Summary

1. Introduction
2. Hypernuclear structure
3. YN and NN interactions
4. Weak hypernuclear decay
5. Weak decay modes of Λ -hypernuclei
 - Mesonic decay
 - Non-mesonic decay
 - One-body induced ($\Lambda N \rightarrow NN$)
 - Two-body induced ($\Lambda NN \rightarrow NNN$)
 - Decay of polarized Λ -hypernuclei

6. Theoretical models for weak hypernuclear decay
 - Wave-function method
 - Polarization propagatore method
 - i) Phenomenological approach
 - ii) Microscopic approach
7. Experiment versus theory
8. The ratio Γ_n/Γ_p
9. s -shell hypernuclei and $\Delta I = 1/2$ rule
10. Non-mesonic decay of polarized Λ -hypernuclei

Theoretical Models for the decay rates

Wave-function Method

Weak effective Hamiltonian for $\Lambda \rightarrow \pi N$ decay:

$$\mathcal{H}_{\Lambda\pi N}^W = iGm_\pi^2 \bar{\psi}_N (A + B\gamma_5) \vec{\tau} \cdot \vec{\phi}_\pi \psi_\Lambda,$$

where $G = 2.211 \cdot 10^{-7}/m_\pi^2$, $A = 1.06$ (PV amplitude) and $B = -7.10$ (PC amplitude) are **fixed on the free Λ decay**. To enforce the $\Delta I = 1/2$ rule the hyperon is assumed to be an **isospin spurion** with $I = 1/2$, $I_z = -1/2$.

In non-relativistic approximation, the **free Λ decay width**

$\Gamma_\Lambda^{\text{free}} = \Gamma_{\pi^-}^{\text{free}} + \Gamma_{\pi^0}^{\text{free}}$ is:

$$\Gamma_\alpha^{\text{free}} = c_\alpha (Gm_\pi^2)^2 \int \frac{d\vec{q}}{(2\pi)^3 2\omega(\vec{q})} 2\pi \delta[E_\Lambda - \omega(\vec{q}) - E_N] \left(S^2 + \frac{P^2}{m_\pi^2} q^2 \right),$$

with $c_\alpha = 1$ for Γ_{π^0} and $c_\alpha = 2$ for Γ_{π^-} , $S = A$, $P = m_\pi B/(2m_N)$.

One finds:

$$\Gamma_{\alpha}^{\text{free}} = c_{\alpha} (Gm_{\pi}^2)^2 \frac{1}{2\pi} \frac{m_N q_{\text{c.m.}}}{m_A} \left(S^2 + \frac{P^2}{m_{\pi}^2} q_{\text{c.m.}}^2 \right)$$

which reproduces the observed rates. $q_{\text{c.m.}} \simeq 100$ MeV is the pion momentum in the center-of-mass frame.

Finite nucleus

$$\text{Mesonic width } \Gamma_M = \Gamma_{\pi^-} + \Gamma_{\pi^0}$$

$$\begin{aligned} \Gamma_\alpha = c_\alpha (Gm_\pi^2)^2 \sum_{N \neq F} \int \frac{d\vec{q}}{(2\pi)^3} \frac{2\pi \delta[E_\Lambda - \omega(\vec{q}) - E_N]}{2\omega(\vec{q})} \\ \times \left\{ S^2 \left| \int d\vec{r} \phi_\Lambda(\vec{r}) \phi_\pi(\vec{q}, \vec{r}) \phi_N^*(\vec{r}) \right|^2 \right. \\ \left. + \frac{P^2}{m_\pi^2} \left| \int d\vec{r} \phi_\Lambda(\vec{r}) \vec{\nabla} \phi_\pi(\vec{q}, \vec{r}) \phi_N^*(\vec{r}) \right|^2 \right\} \end{aligned}$$

The Λ and nucleon wave functions ϕ_Λ and ϕ_N obtainable within a **shell model**. Pion wave function ϕ_π corresponds to outgoing wave solution of the Klein–Gordon eq. with πN optical potential V_{opt} :

$$\left\{ \vec{\nabla}^2 - m_\pi^2 - 2\omega V_{\text{opt}}(\vec{r}) + [\omega - V_C(\vec{r})]^2 \right\} \phi_\pi(\vec{q}, \vec{r}) = 0$$

Non-mesonic width

Weak transition $\Lambda N \rightarrow NN$ proceeds via the exchange of virtual mesons of the pseudoscalar (π , η and K) and vector (ρ , ω and K^*) octets.

OPE non-relativistic $\Lambda N \rightarrow NN$ transition potential:

$$V_\pi(\vec{q}) = -Gm_\pi^2 \frac{g_{NN\pi}}{2m_N} \left(A + \frac{B}{2\bar{m}} \vec{\sigma}_1 \cdot \vec{q} \right) \frac{\vec{\sigma}_2 \cdot \vec{q}}{q^2 + m_\pi^2} \vec{\tau}_1 \cdot \vec{\tau}_2$$

where $\bar{m} = (m_\Lambda + m_N)/2$.

Large momenta ($\simeq 420$ MeV) exchanged in the $\Lambda N \rightarrow NN$ transition:

\implies heavier mesons contribute, e.g.

$$V_\rho(\vec{q}) = Gm_\pi^2 \left[g_{NN\rho}^V - \frac{(\alpha + \beta)(g_{NN\rho}^V + g_{NN\rho}^T)}{4m_{\bar{m}}m} \right] (\vec{\sigma}_1 \times \vec{q}) \cdot (\vec{\sigma}_2 \times \vec{q}) \alpha \\ + i \frac{\epsilon(g_{NN\rho}^V + g_{NN\rho}^T)}{2m_{\bar{m}}} (\vec{\sigma}_1 \times \vec{\sigma}_2) \cdot \vec{q} \left[\frac{\vec{\tau}_1 \cdot \vec{\tau}_2}{q^2 + m_\rho^2} \right]$$

Weak coupling constants α , β and ϵ must be evaluated theoretically.

Most general **OME potential**

$$V(\vec{r}) = \sum_m V_m(\vec{r}) = \sum_m \sum_\alpha V_m^\alpha(r) \hat{O}^\alpha(\hat{r}) \hat{I}_m,$$

where $m = \pi, \eta, K, \rho, \omega, K^*$; the spin operator \hat{O}^α is:

$$\hat{O}^\alpha(\hat{r}) = \begin{cases} \hat{1} & \text{central spin – independent,} \\ \vec{\sigma}_1 \cdot \vec{\sigma}_2 & \text{central spin – dependent,} \\ S_{12}(\hat{r}) & \text{tensor,} \\ \vec{\sigma}_2 \cdot \hat{r} & \text{PV for pseudoscalar mesons,} \\ (\vec{\sigma}_1 \times \vec{\sigma}_2) \cdot \hat{r} & \text{PV for vector mesons,} \end{cases}$$

with

$$S_{12}(\hat{r}) = 3(\vec{\sigma}_1 \cdot \hat{r})(\vec{\sigma}_2 \cdot \hat{r}) - \vec{\sigma}_1 \cdot \vec{\sigma}_2$$

The isospin operator \hat{I}_m is:

$$\hat{I}_m = \begin{cases} \hat{1} & \text{isoscalars mesons } (\eta, \omega) \\ \vec{\tau}_1 \cdot \vec{\tau}_2 & \text{isovector mesons } (\pi, \rho) \\ \hat{1} \pm \vec{\tau}_1 \cdot \vec{\tau}_2 & \text{isodoublet mesons } (K, K^*) \end{cases}$$

One-body induced non-mesonic decay rate

(initial hypernucleus at rest)

$$\Gamma_1 = \int \frac{d\vec{p}_1}{(2\pi)^3} \int \frac{d\vec{p}_2}{(2\pi)^3} 2\pi \delta(\text{E.C.}) \overline{\sum} |\mathcal{M}(\vec{p}_1, \vec{p}_2)|^2,$$

with

$$\delta(\text{E.C.}) = \delta \left(m_H - E_R - 2m_N - \frac{p_1^2}{2m_N} - \frac{p_2^2}{2m_N} \right);$$

and

$$\mathcal{M}(\vec{p}_1, \vec{p}_2) \equiv \langle \Psi_R; N(\vec{p}_1) N(\vec{p}_2) | \hat{T}_{\Lambda N \rightarrow NN} | \Psi_H \rangle$$

The sum $\overline{\sum}$ indicates average over the third component of the hypernuclear total spin and sum over quantum numbers of the residual system and over spin and isospin third components of the outgoing nucleons. In shell model calculations the weak-coupling scheme is used to describe the hypernuclear wave function Ψ_H .

The many-body transition amplitude $\mathcal{M}(\vec{p}_1, \vec{p}_2)$ is expressed in terms of two-body amplitudes $\langle NN|V|AN\rangle$ of the OME potential.

Remarks:

- Λ decays from an orbital angular momentum $l = 0$ state
- One can isolate the contributions of neutron- and proton-induced transitions
- NN final state interactions and AN correlations can also be implemented

Polarization Propagator Method

Weak effective hamiltonian for $\Lambda \rightarrow \pi N$ decay (again):

$$\mathcal{H}_{\Lambda\pi N}^W = iGm_\pi^2 \bar{\psi}_N (A + B\gamma_5) \vec{\tau} \cdot \vec{\phi}_\pi \psi_\Lambda.$$

Alternative (and equivalent) approach to the calculation of the hyperon width: start from imaginary part of the Λ self-energy:

$$\Gamma_\Lambda = -2 \text{Im} \Sigma_\Lambda$$

in non-relativistic limit:

$$\Sigma_\Lambda(k) = 3i(Gm_\pi^2)^2 \int \frac{d^4q}{(2\pi)^4} \left(S^2 + \frac{P^2}{m_\pi^2} \vec{q}^2 \right) F_\pi^2(q) G_N(k-q) G_\pi(q)$$

Nucleon propagator in the medium (includes the effect of binding):

$$G_N(\mathbf{p}) = \frac{\theta(|\vec{p}| - k_F)}{p_0 - E_N(\vec{p}) - V_N + i\epsilon} + \frac{\theta(k_F - |\vec{p}|)}{p_0 - E_N(\vec{p}) - V_N - i\epsilon}$$

Pion propagator reads:

$$G_\pi(q) = \frac{1}{q_0^2 - \vec{q}^2 - m_\pi^2 - \Sigma_\pi^*(q)}$$

Pion self-energy $\Sigma_\pi^*(q)$ evaluated in nuclear medium within RPA approximation and beyond.

the Λ self-energy is modified in the medium:

$$\begin{aligned} \Gamma_\Lambda(\vec{k}, \rho) = & -6(Gm_\pi^2)^2 \int \frac{d\vec{q}}{(2\pi)^3} \theta(|\vec{k} - \vec{q}| - k_F) \\ & \times \theta(k_0 - E_N(\vec{k} - \vec{q}) - V_N) \text{Im}[\alpha(q)]_{q_0=k_0 - E_N(\vec{k} - \vec{q}) - V_N} \end{aligned}$$

$$\alpha(\mathbf{q}) = \left(S^2 + \frac{P^2}{m_\pi^2} \vec{q}^2 \right) F_\pi^2(\mathbf{q}) G_\pi^0(\mathbf{q}) + \frac{\tilde{S}^2(\mathbf{q}) U_L(\mathbf{q})}{1 - V_L(\mathbf{q}) U_L(\mathbf{q})} \\ + \frac{\tilde{P}_L^2(\mathbf{q}) U_L(\mathbf{q})}{1 - V_L(\mathbf{q}) U_L(\mathbf{q})} + 2 \frac{\tilde{P}_T^2(\mathbf{q}) U_T(\mathbf{q})}{1 - V_T(\mathbf{q}) U_T(\mathbf{q})}$$

the effective weak (\tilde{S} , \tilde{P}_L , \tilde{P}_T) and strong (V_L , V_T) interactions include π - and ρ -exchange plus short range repulsive correlations

$U_L(\mathbf{q})$ and $U_T(\mathbf{q})$ contain the Lindhard functions (particle-hole propagator) for p - h and Δ - h excitations and the irreducible $2p$ - $2h$ polarization

propagator:

$$U_{L,T}(\mathbf{q}) = U^{ph}(\mathbf{q}) + U^{\Delta h}(\mathbf{q}) + U_{L,T}^{2p2h}(\mathbf{q})$$

NB Decay width depends upon nuclear matter density

$$\rho = 2k_F^3/3\pi^2.$$

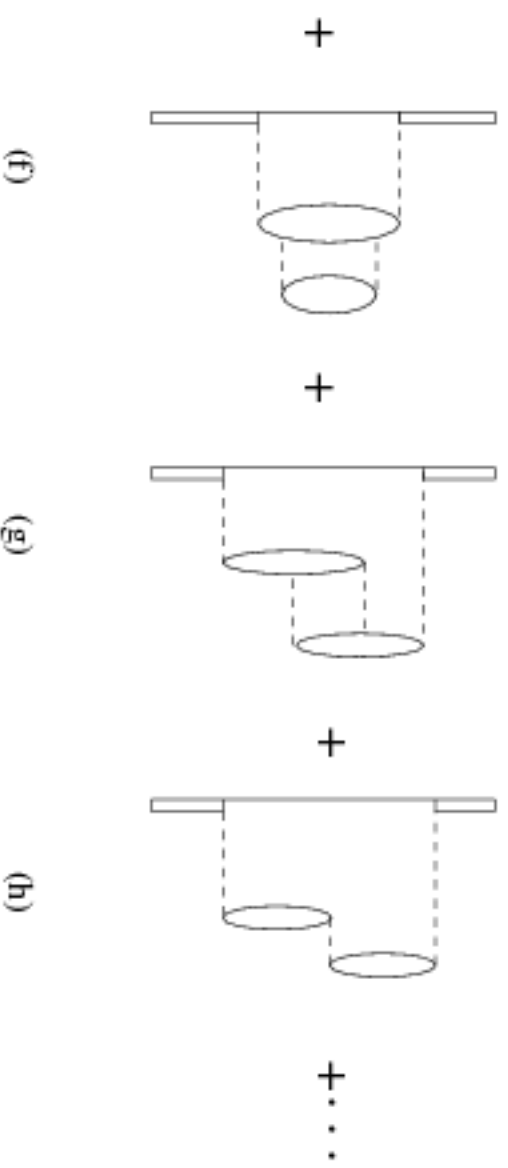
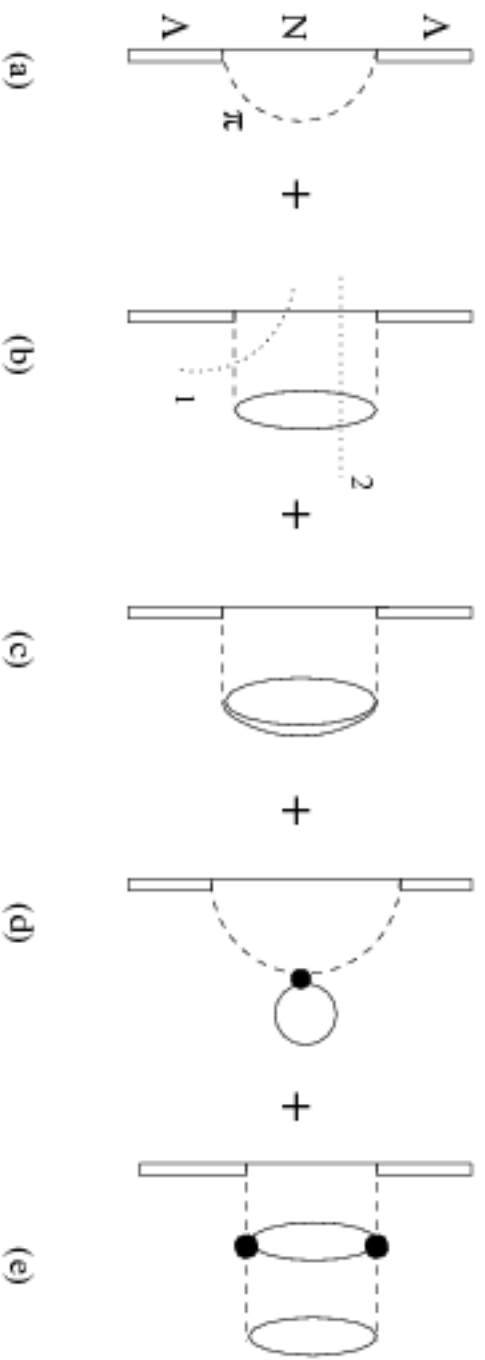


Figure 1: Lowest order terms for the Λ self-energy in nuclear matter.

Two different approaches for the evaluation of $U_{L,T}^{2p2h}(q)$:

A. Phenomenological

B. Microscopic

$\text{Im } \alpha(q)$ develops various contributions:

$$\text{Im} \frac{U_{L,T}(q)}{1 - V_{L,T}(q)U_{L,T}(q)} = \frac{\text{Im } U^{ph}(q) + \text{Im } U^{\Delta h}(q) + \text{Im } U_{L,T}^{2p2h}(q)}{|1 - V_{L,T}(q)U_{L,T}(q)|^2}$$

the three terms representing different decay mechanisms of the hypernucleus:

$$\Gamma_M \propto \text{Im } U^{\Delta h} \quad (\text{part of mesonic width})$$

$$\Gamma_1 \propto \text{Im } U^{ph} \quad (\text{non-mesonic, 1-body induced decay width})$$

$$\Gamma_2 \propto \text{Im } U^{2p2h} \quad (\text{non-mesonic, 2-body induced + part of mesonic width})$$

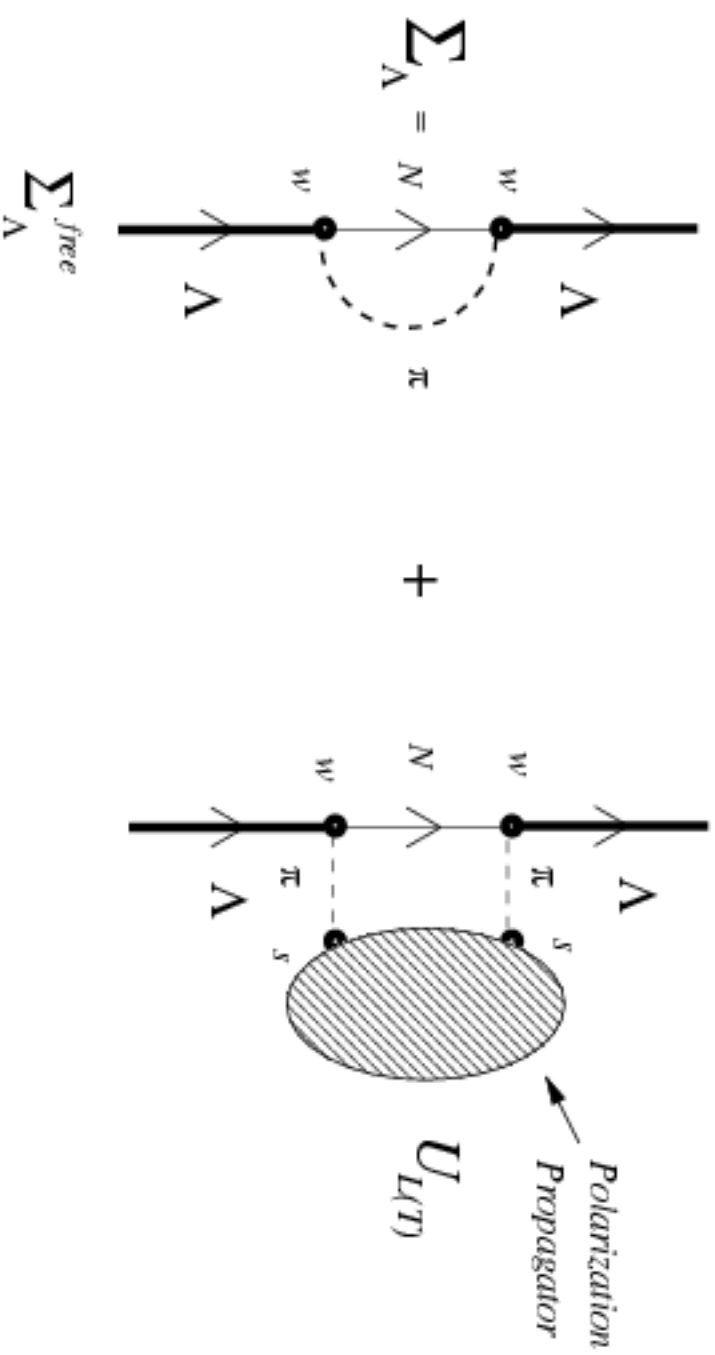


Figure 2: Schematic representation of the total Λ self-energy in terms of the π self-energy and polarization insertions; in the vertices: w =weak, s =strong.



Figure 3: One-body induced decay process in the language of particle-hole states.

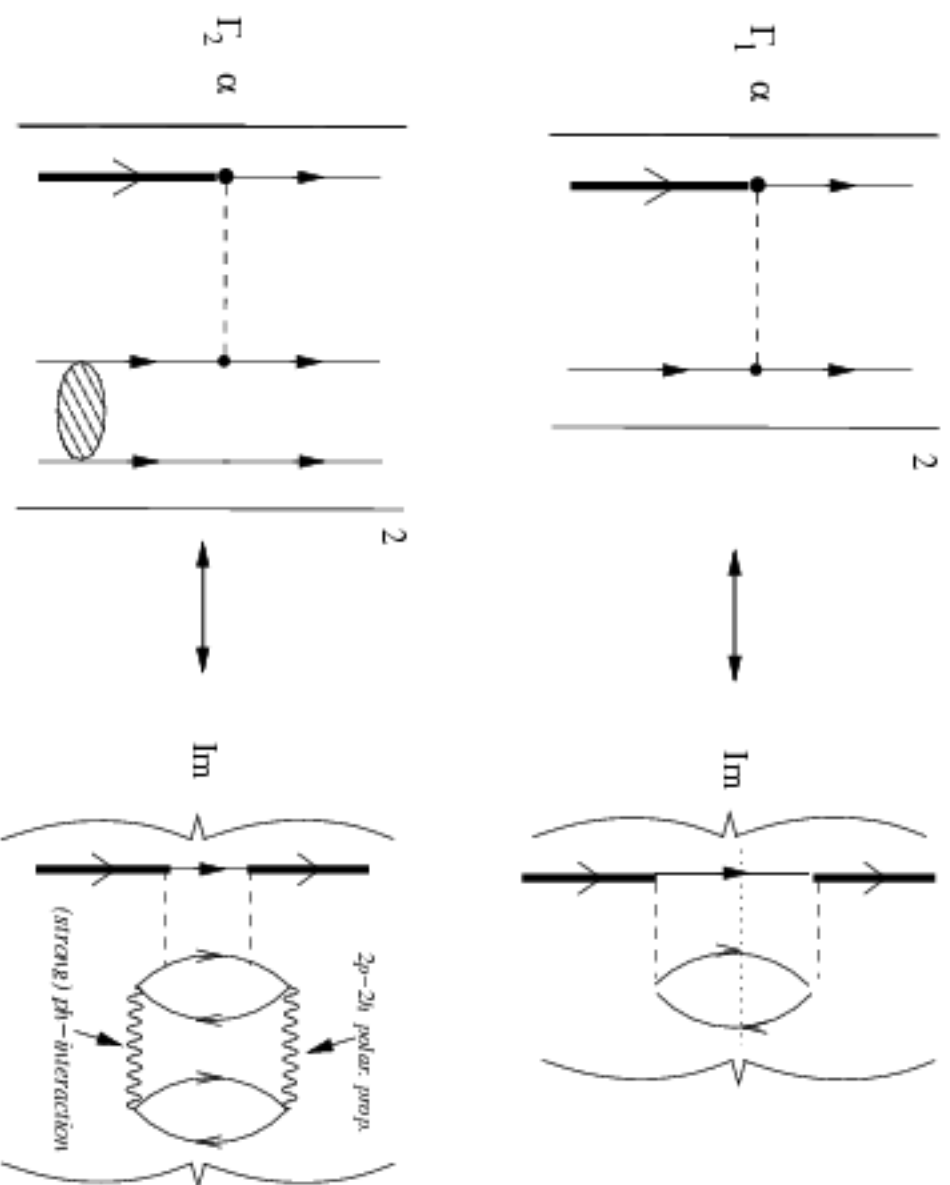


Figure 4: Schematic relation between the one-body (upper panel) and two-body (lower panel) Λ decay amplitudes and the Imaginary part of specific contributions to the Λ self-energy.

Spin-isospin $NN \rightarrow NN$ and $NN \rightarrow NN$ interactions

The $NN \rightarrow NN$ interaction can be described through the effective potential:

$$G(r) = g(r)V(r).$$

Here $g(r)$ is a two-body correlation function, which vanishes as $r \rightarrow 0$ and goes to 1 as $r \rightarrow \infty$.

$V(r)$ is the meson exchange potential, which contains π and ρ exchange:

$$V = V_\pi + V_\rho.$$

A practical and realistic form for $g(r)$ is [Oset, Toki, Weise, Phys.Rep. 83 (1982) 281]:

$$g(r) = 1 - j_0(q_c r),$$

where j_0 is the Bessel spherical function of order 0. With $q_c = m_\omega \simeq 780$ MeV one gets a good reproduction of realistic NN correlation functions obtained from G -matrix calculations. The inverse of q_c is indicative of the hard core radius of the interaction.

Using this correlation function it is easy to get the effective interaction:

$$G_{NN \rightarrow NN}(q) = V_\pi(q) + V_\rho(q) + \frac{f_\pi^2}{m_\pi^2} \{g_L(q)\hat{q}_i\hat{q}_j + g_T(q)(\delta_{ij} - \hat{q}_i\hat{q}_j)\} \sigma_i\sigma_j\vec{\tau} \cdot \vec{\tau}$$

where **correlations** are embodied in the functions g_L and g_T .

The spin-isospin $NN \rightarrow NN$ interaction can be separated into a spin-longitudinal and a spin-transverse parts:

$$G_{NN \rightarrow NN}(q) = \{V_L(q)\hat{q}_i\hat{q}_j + V_T(q)(\delta_{ij} - \hat{q}_i\hat{q}_j)\} \sigma_i\sigma_j\vec{\tau} \cdot \vec{\tau}$$

where:

$$V_L(q) = \frac{f_\pi^2}{m_\pi^2} \{ \vec{q}^2 F_\pi^2(q) G_\pi^0(q) + g_L(q) \}$$

$$V_T(q) = \frac{f_\pi^2}{m_\pi^2} \{ \vec{q}^2 C_\rho F_\rho^2(q) G_\rho^0(q) + g_T(q) \}$$

In the above, F_π and F_ρ are the πNN and ρNN form factors, G_π and G_ρ are the corresponding free meson propagators: $G_m^0 = 1/(q_0^2 - \vec{q}^2 - m_m^2)$.

The $AN \rightarrow NN$ transition potential, modified by the effect of the strong AN correlations, splits into a P -wave (again spin-longitudinal and spin-transverse):

$$G_{AN \rightarrow NN}(q) = \left\{ \tilde{P}_L(q) \hat{q}_i \hat{q}_j + \tilde{P}_T(q) (\delta_{ij} - \hat{q}_i \hat{q}_j) \right\} \sigma_i \sigma_j \vec{\tau} \cdot \vec{\tau}$$

with:

$$\tilde{P}_L(q) = \frac{f_\pi}{m_\pi} \frac{P}{m_\pi} \left\{ \vec{q}^2 F_\pi^2(q) G_\pi^0(q) + g_L^\Delta(q) \right\}$$

$$\tilde{P}_T(q) = \frac{f_\pi}{m_\pi} \frac{P}{m_\pi} g_T^\Delta(q)$$

and an S -wave part:

$$\tilde{S}(q) = \frac{f_\pi}{m_\pi} S \left\{ F_\pi^2(q) G_\pi^0(q) - \tilde{F}_\pi^2(q) \tilde{G}_\pi^0(q) \right\} |\vec{q}|$$

A. Phenomenological $2p2h$ propagator

[Ref.: A.Ramos, E.Oset, L.L.Salcedo, PRC 50 (1994), 2314
W.M.Alberico, A.De Pace, G.Garbarino, A.Ramos, PRC 61 (2000) 044314]

Momentum dependence of the imaginary part of $U_{L,T}^{2p2h}$ obtained from available phase-space:

$$\text{Im } U_{L,T}^{2p2h}(q_0, \vec{q}; \rho) = \frac{P(q_0, \vec{q}; \rho)}{P(m_\pi, \vec{0}; \rho_{\text{eff}})} \text{Im } U_{L,T}^{2p2h}(m_\pi, \vec{0}; \rho_{\text{eff}})$$

where $\rho_{\text{eff}} = 0.75\rho$ and

$$P(q_0, \vec{q}; \rho) \propto \int \frac{d^4k}{(2\pi)^4} \text{Im } U^{ph}\left(\frac{q}{2} + k; \rho\right) \text{Im } U^{ph}\left(\frac{q}{2} - k; \rho\right) \theta\left(\frac{q_0}{2} \pm k_0\right)$$

Moreover $\text{Im } U_{L,T}^{2p2h}(m_\pi, \vec{0}; \rho_{\text{eff}})$ can be fixed through the p -wave pion-nucleus optical potential.

Local Density Approximation

Calculation of the widths is performed in nuclear matter and extended to finite nuclei via the LDA.

A local Fermi sea of nucleons is introduced

$$k_F(\vec{r}) = \left\{ \frac{3}{2} \pi^2 \rho_A(\vec{r}) \right\}^{1/3}$$

Nuclear density assumed to be a Fermi distribution.

Decay width in finite nuclei is then obtained by:

$$\Gamma_\Lambda = \int d\vec{k} |\tilde{\psi}_\Lambda(\vec{k})|^2 \Gamma_\Lambda(\vec{k})$$

where:

$$\Gamma_\Lambda(\vec{k}) = \int d\vec{r} |\psi_\Lambda(\vec{r})|^2 \Gamma_\Lambda[\vec{k}, \rho(\vec{r})]$$

and $|\tilde{\psi}_\Lambda(\vec{k})|^2$ is Λ momentum distribution.

The Λ wave function $\psi_\Lambda(\vec{r})$ is obtained from a Woods–Saxon Λ -nucleus potential, which exactly reproduces the first two single particle eigenvalues (s and p Λ levels) of the hypernucleus under analysis.

B. Microscopic approach

Microscopic evaluation of the 2p-2h propagator within the so-called bosonic loop expansion. For details see:

W.M.Alberico, A.De Pace, G.Garbarino, R.Cenni, NPA 668 (2000) 113

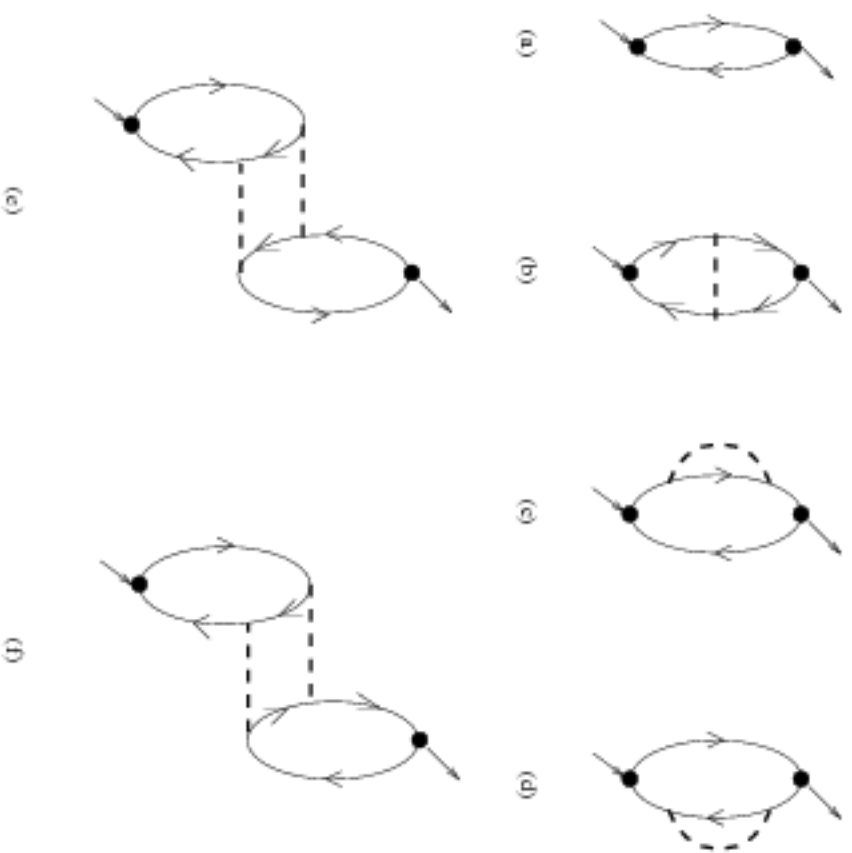


Figure 5: Feynman diagrams for the polarization propagator in OBL: (a) particle-hole; (b) exchange; (c) and (d) self-energy-type; (e) and (f) correlation diagrams. Only the first contribution to the ring expansion has been drawn. The dashed lines represent ring-dressed pion propagators.

Experiment versus theory

Partial and total decay rates

Two ingredients are crucial to the determination of partial and total decay widths:

- Short range correlations in NN interactions (g') and in $\Lambda N \rightarrow NN$ (g'_Λ) transition potential
- Choice of the Λ wave-function

Short range correlations are only partly known from existing phenomenology: in NN channel g' was constrained by, e.g., quenching of Gamow-Teller resonance and quasi-elastic transverse electron-nucleus scattering (realistic values within ordinary RPA scheme: $g' = 0.6 \div 0.7$).
No information instead is available on g'_Λ .

\Rightarrow Fix both parameters on the basis of agreement with experimental decay widths.

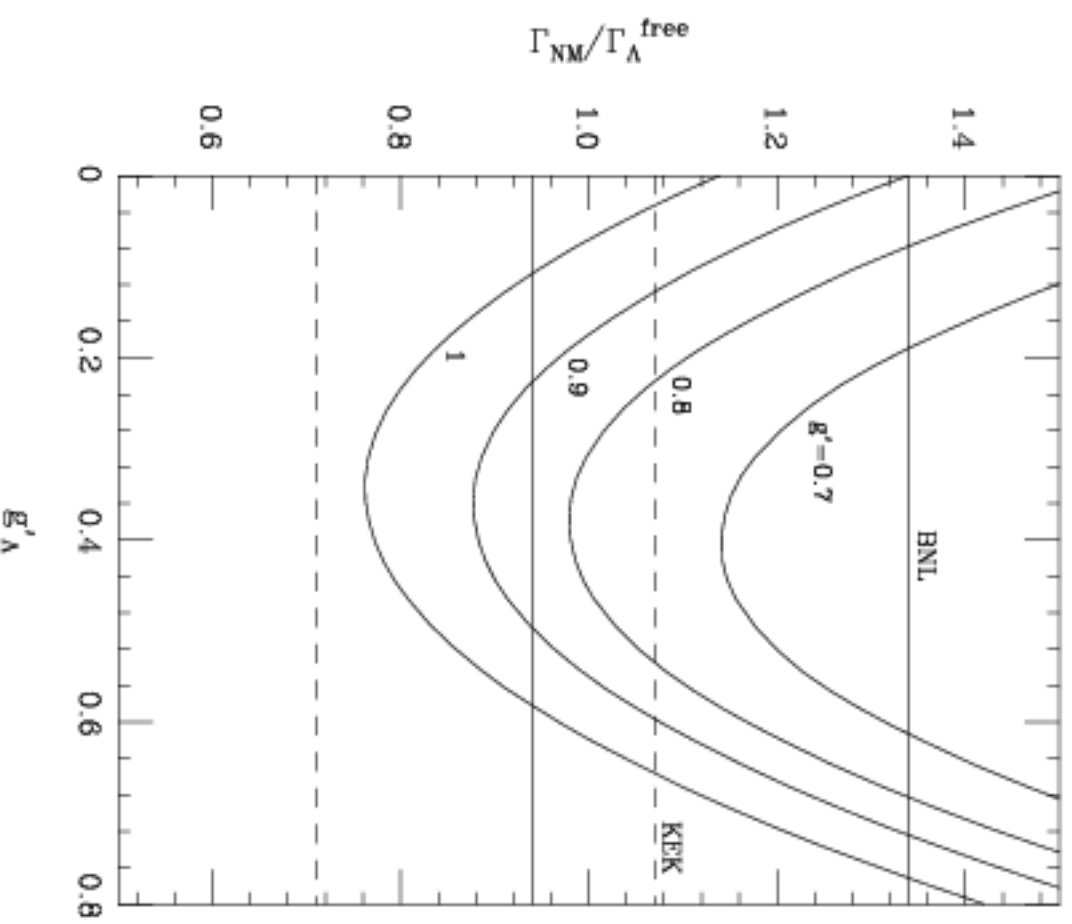


Figure 6: Dependence of the non-mesonic width on the Landau parameters g'_{Λ} and g'_{Λ} for ^{12}C . The experimental value from BNL[1991] (KEK[1995]) lies

The **Λ wave function** sensibly affects the calculation of decay rates: different examples are obtained with Woods-Saxon wave functions of [Dover, Gal, Millener, PRC 38 (1988) 2700], Harmonic Oscillator wave function with empirical frequency ω obtained from $s - p$ energy shift [Hasegawa, et al., PRC 53 (1996) 1210], wave functions from a Woods-Saxon potential that reproduces the s and p Λ -levels [Alberico, De Pace, Garbarino, Ramos, PRC 61 (2000) 044314].

Note: Mesonic width almost insensitive.

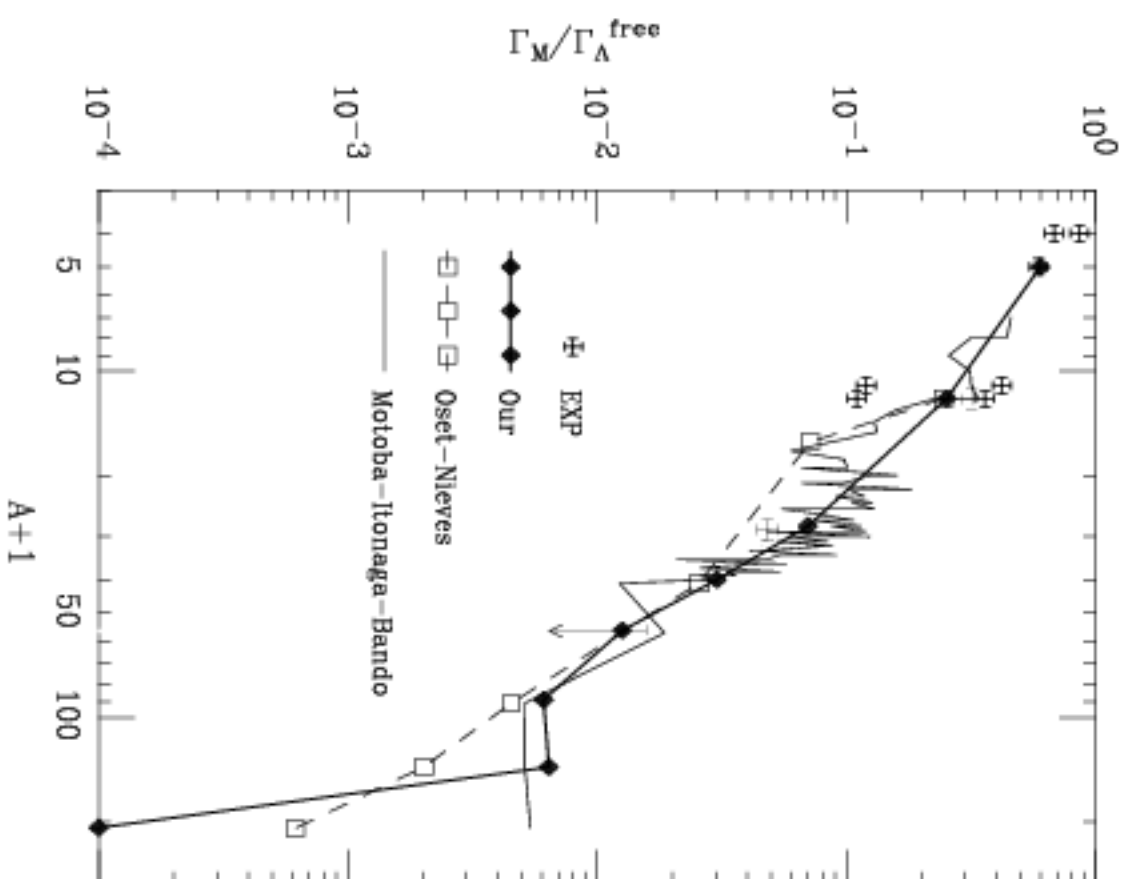


Figure 7: Mesonic width

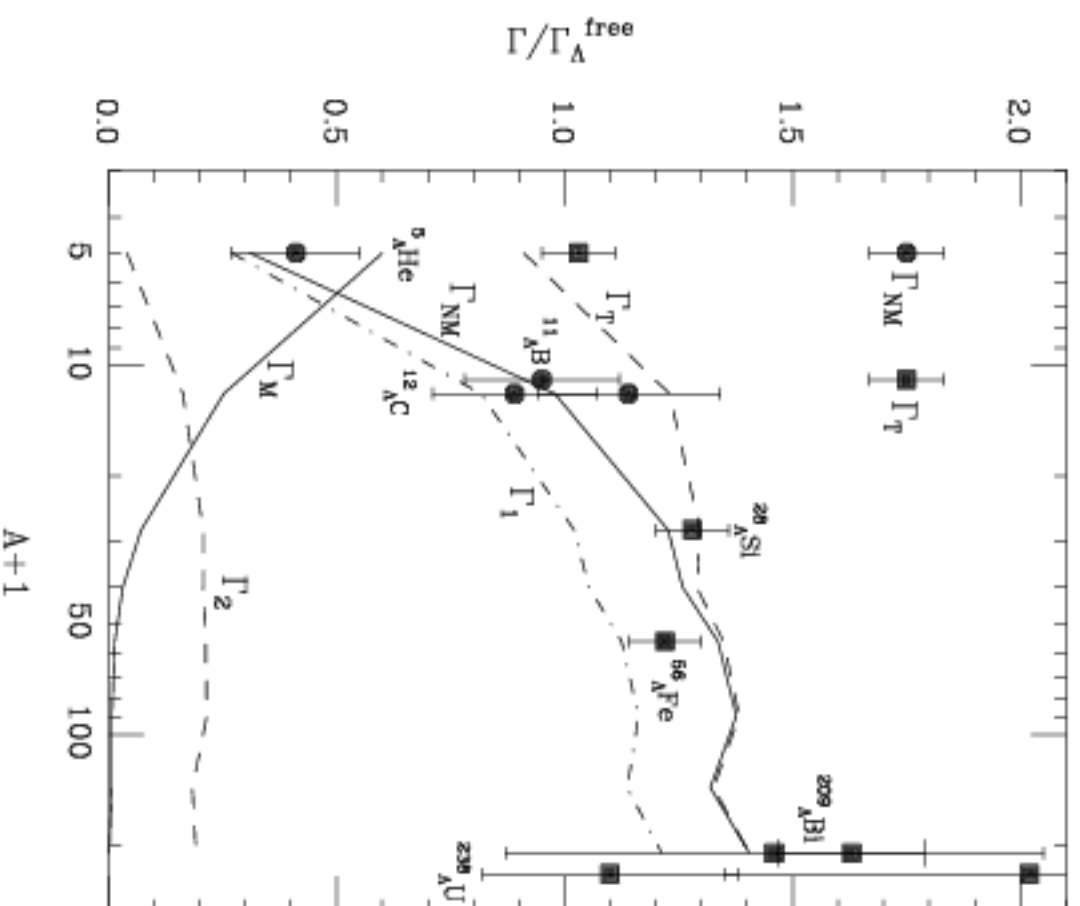


Figure 8: Partial Λ decay widths

Table 1: Mass dependence of the hypernuclear weak decay rates.

| ${}^{A+1}_AZ$ | Γ_M | Γ_1 | Γ_2 | Γ_T |
|-----------------------|-------------------|------------|------------|------------|
| ${}^5_A\text{He}$ | 0.60 | 0.27 | 0.04 | 0.91 |
| ${}^{12}_A\text{C}$ | 0.25 | 0.82 | 0.16 | 1.23 |
| ${}^{28}_A\text{Si}$ | 0.07 | 1.02 | 0.21 | 1.30 |
| ${}^{40}_A\text{Ca}$ | 0.03 | 1.05 | 0.21 | 1.29 |
| ${}^{56}_A\text{Fe}$ | 0.01 | 1.12 | 0.21 | 1.35 |
| ${}^{89}_A\text{Y}$ | $6 \cdot 10^{-3}$ | 1.16 | 0.22 | 1.38 |
| ${}^{139}_A\text{La}$ | $6 \cdot 10^{-3}$ | 1.14 | 0.18 | 1.33 |
| ${}^{208}_A\text{Pb}$ | $1 \cdot 10^{-4}$ | 1.21 | 0.19 | 1.40 |

The ratio Γ_n/Γ_p

In OPE approximation, by assuming the $\Delta I = 1/2$ rule,

$$[\Gamma_n/\Gamma_p]^{\text{OPE}} \simeq 0.05 \div 0.20$$

for all considered systems.

For pure $\Delta I = 3/2$ transitions the OPE ratio can increase up to about 0.5, but the OPE model reproduces fairly well the rates $\Gamma_1 = \Gamma_n + \Gamma_p$ for light and medium hypernuclei.

Other ingredients to take into account:

- heavier mesons ($\rho, K, K^*, \omega, \eta$)
- direct quark mechanism
- two-nucleon induced mechanism
- nucleon final state interactions

Calculations with $\Lambda N \rightarrow NN$ transition potentials including **heavy-meson-exchange** (e.g. K) or **direct quark contributions** have improved the situation.

The analysis of the ratio Γ_n/Γ_p is influenced by the **two-nucleon induced process** $\Lambda NN \rightarrow NNN$: by assuming quasi-deuteron absorption for the emitted meson, the three-body process are $\Lambda np \rightarrow nnp$ and a considerable fraction of neutrons could come from this channel in addition to $\Lambda n \rightarrow nn$ and $\Lambda p \rightarrow np$.

However the inclusion of the new channel would bring to extract from the experiment even larger values for the Γ_n/Γ_p ratios.

Table 2: Γ_n/Γ_p ratio.

| Ref. and Model | ${}^5_\Lambda\text{He}$ | ${}^{12}_\Lambda\text{C}$ |
|---|-------------------------|---------------------------|
| Itonaga <i>et al.</i> 1998 ($\pi + 2\pi/\rho + 2\pi/\sigma$) | | 0.36 |
| Sasaki <i>et al.</i> 2000 ($\pi + K + \text{DQ}$) | 0.701 | |
| Jun <i>et al.</i> 2001 (OPE + 4BPI) | 1.30 | 1.14 |
| Jido <i>et al.</i> 2001 ($\pi + K + 2\pi + \omega$) | | 0.53 |
| Parreño–Ramos 2001 ($\pi + \rho + K + K^* + \omega + \eta$) | 0.343 \div 0.457 | 0.288 \div 0.341 |
| Exp KEK 1995 | | 1.87 $^{+0.67}_{-1.16}$ |
| Exp KEK 1995 | 1.97 \pm 0.67 | |
| Exp KEK 2004 | | 0.87 \pm 0.23 |
| Exp KEK 2004 (with Garbarino <i>et al.</i> analysis) | 0.39 \pm 0.11 | |

Effect of final state interaction (FSI)

on the spectra of emitted nucleons

Nucleon energy/momentum distributions have been calculated by using a Monte Carlo simulation to describe nucleon rescattering inside the nucleus.

[Refs.: Ramos, Vicente-Vacas, Oset, PRC 55 (1997) 735; PRC 66 (2002) 039903 (E); Garbarino, Parreño, Ramos, PRL 91 (2003) 112501, PRC 69 (2004) 054603]

Study of the **nucleon distributions** in the NMWD of ${}^5_\Lambda\text{He}$ and ${}^12_\Lambda\text{C}$ hypernuclei, in particular:

- Single nucleon energy spectra
- NN angular and energy correlations

Main ingredients:

1. Finite nucleus treatment for $\Lambda n \rightarrow nN$
(OME = $\pi + \rho + K + K^* + \omega + \eta$)
[Parreño, Ramos, Bennhold, PRC 56 (1997) 339; Parreño, Ramos, PRC 65 (2002) 015204]
2. Polarization propagator method in LDA for $\Lambda NN \rightarrow nNN$ (correlated OPE)
[Alberico, de Pace, Garbarino, Ramos, PRC 61 (2000) 044314]
3. Intranuclear Cascade calculation

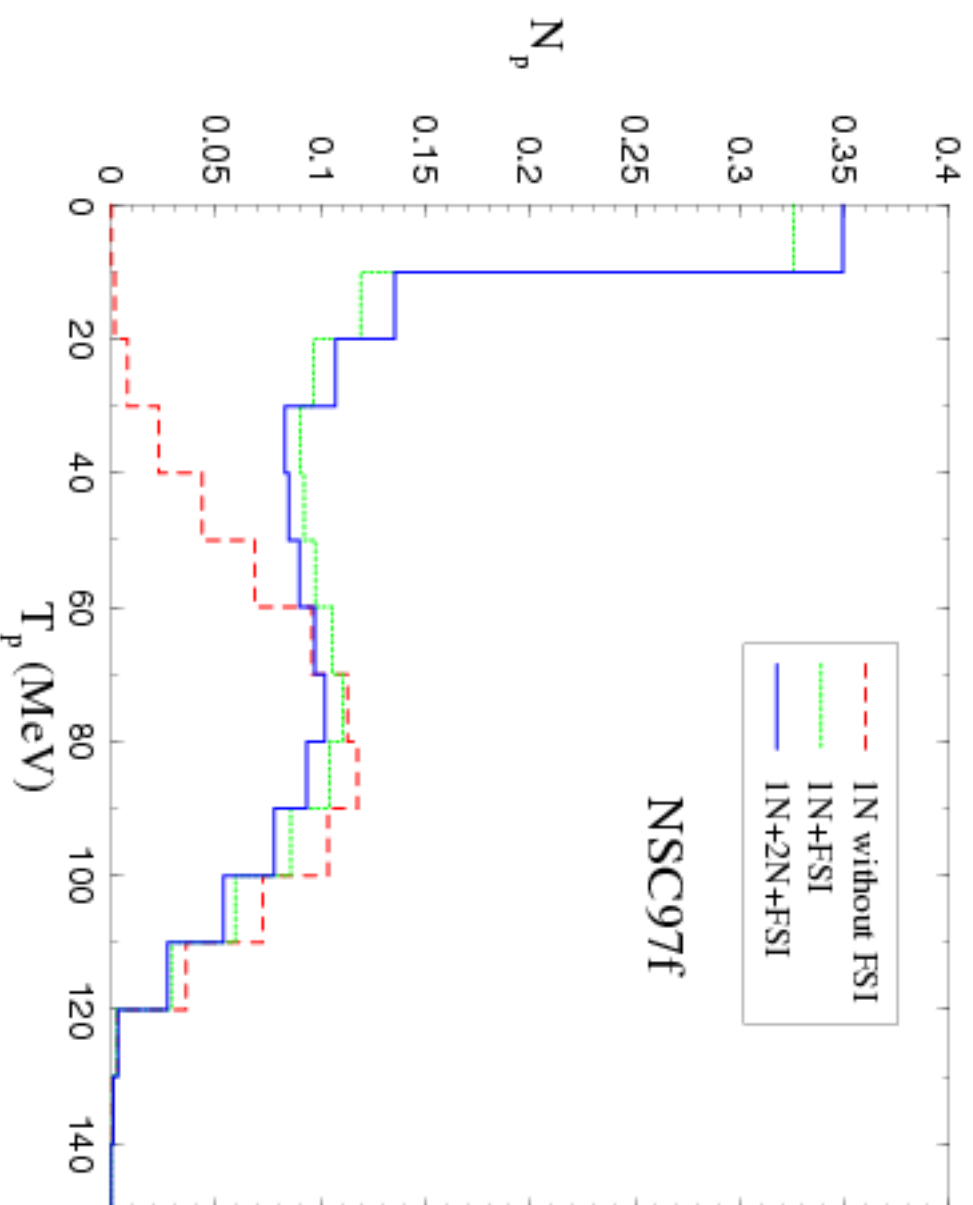


Figure 9: Single-proton kinetic energy spectra for the non-mesonic decay of ${}^5_{\Lambda}\text{He}$
($\Gamma_n/\Gamma_p = 0.46$)

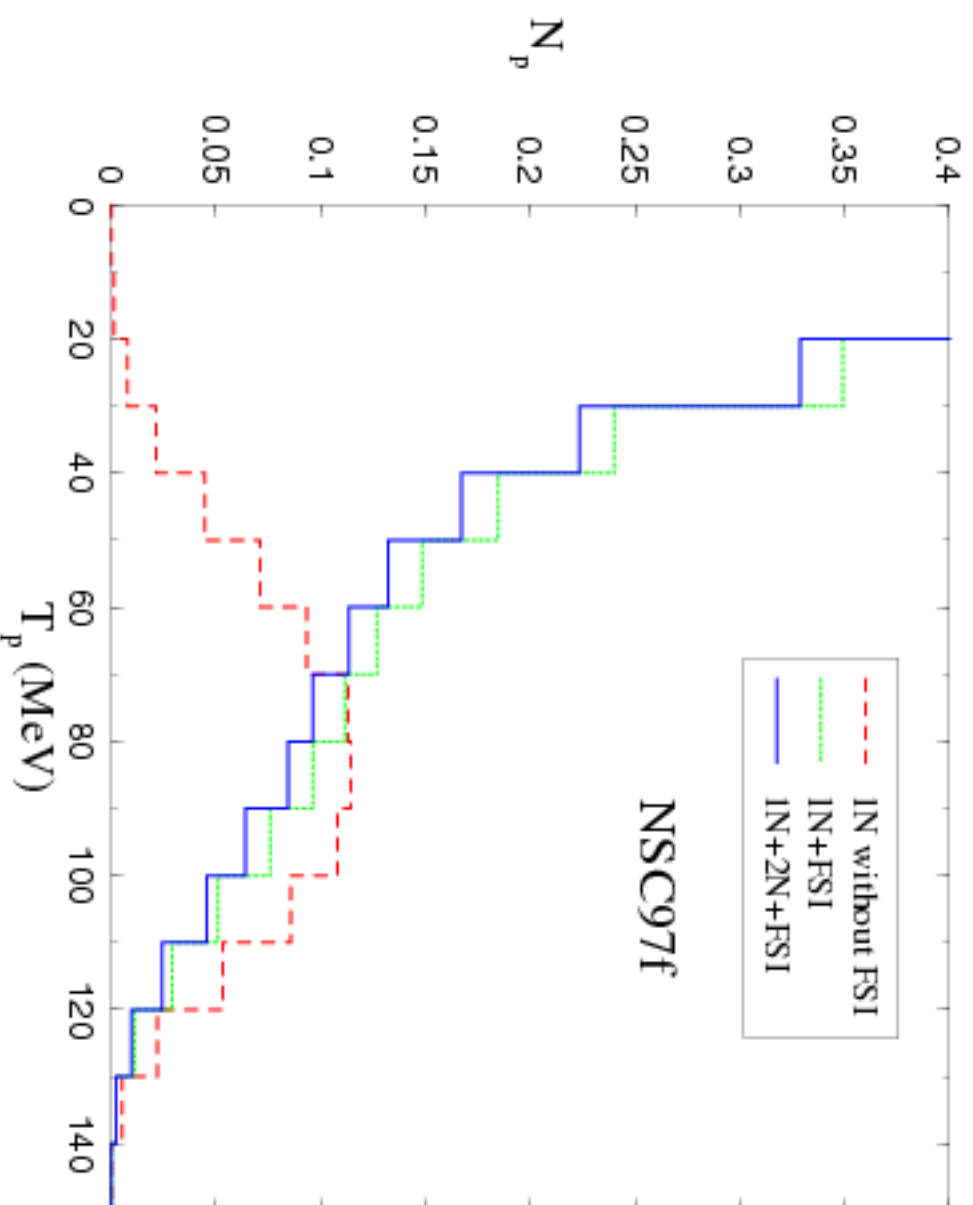


Figure 10: Single-proton kinetic energy spectra for the non-mesonic decay of ^{12}C
 ($\Gamma_n/\Gamma_p = 0.34$)

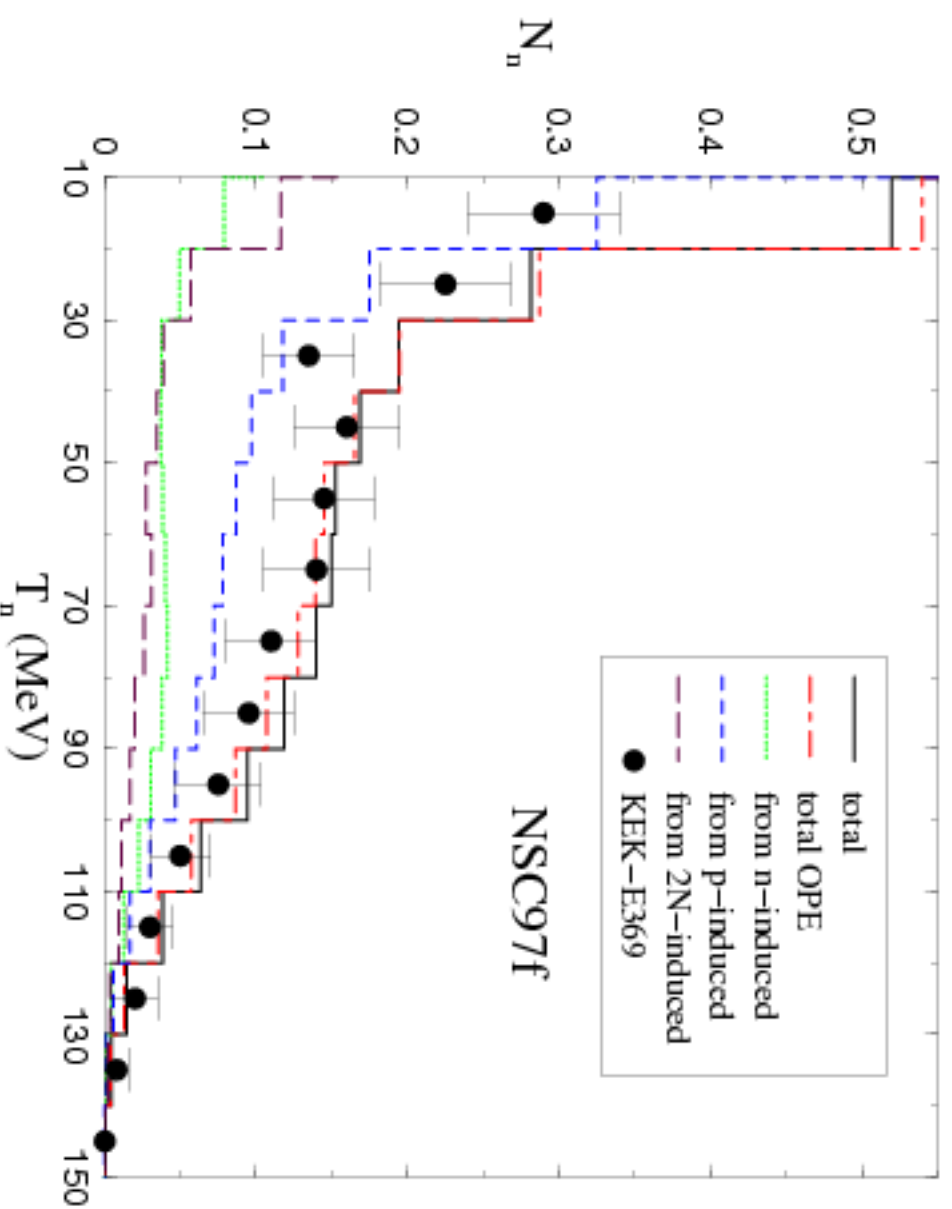


Figure 11: Single-neutron kinetic energy spectra for the non-mesonic decay of $^{12}\text{C}_A$. Data from Kim et al., PRC 68 (2003) 065201.

Number of primary nucleons:

$$\begin{aligned} N_n^{\text{wd}} &\propto 2\Gamma_n + \Gamma_p \\ N_p^{\text{wd}} &\propto \Gamma_p \end{aligned}$$

$$\frac{\Gamma_n}{\Gamma_p} \equiv \frac{1}{2} \left(\frac{N_n^{\text{wd}}}{N_p^{\text{wd}}} - 1 \right)$$

But, due to **FSI**:

$$\frac{\Gamma_n}{\Gamma_p} \neq \frac{1}{2} \left(\frac{N_n}{N_p} - 1 \right) \equiv R_1(T_N^{\text{th}})$$

N_n , N_p are the number of nucleons emitted by the nucleus

Table 3: Predictions for $R_1(T_N^{\text{th}})$ for ${}^5_\Lambda\text{He}$.

| | T_N^{th} (MeV) | | | Γ_n/Γ_p |
|------------------|-------------------------|------|-------------|---------------------|
| | 0 | 30 | 60 | |
| OPE | 0.04 | 0.13 | 0.16 | 0.09 |
| OMF _a | 0.15 | 0.32 | 0.39 | 0.34 |
| OMF _f | 0.19 | 0.40 | 0.49 | 0.46 |

KEK – E462 : $R_1(60\text{MeV}) = 0.6 \pm 0.2$ (preliminary)

[H. Bhang, HYP2003]

${}^5\text{He} - 1\text{N}+2\text{N}$ induced

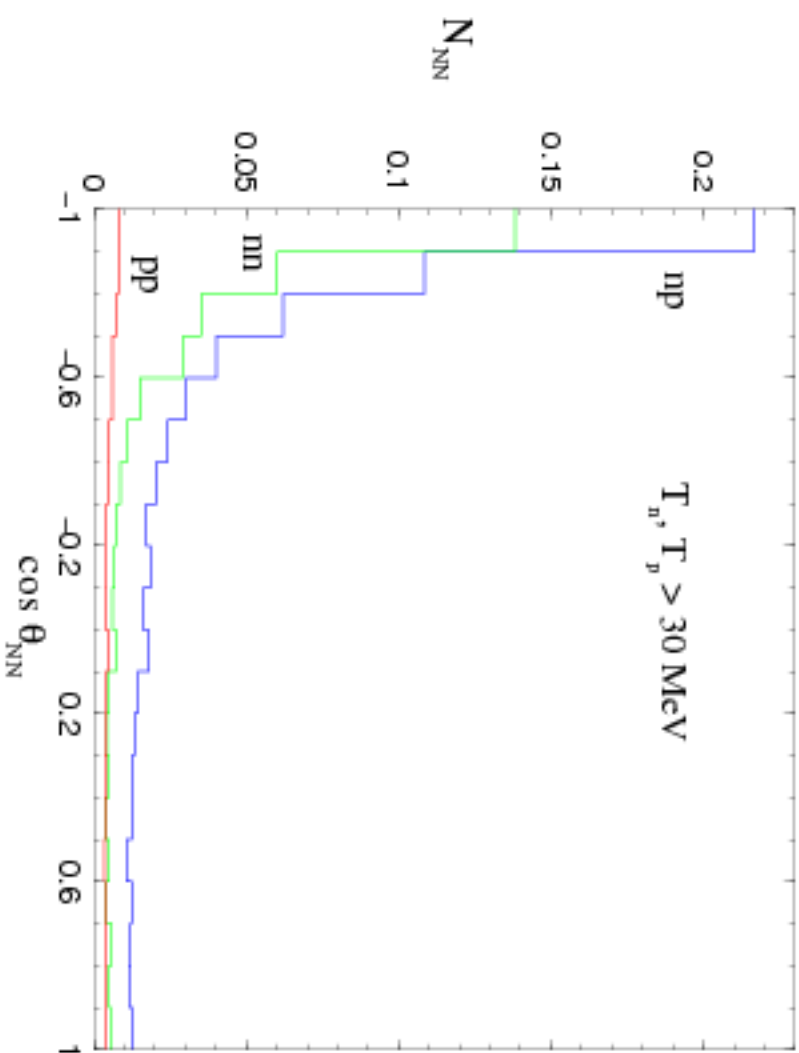


Figure 12: ANGULAR CORRELATIONS: Opening angle distributions of nn , np and pp pairs emitted per NMWD of ${}^5\text{He}$.

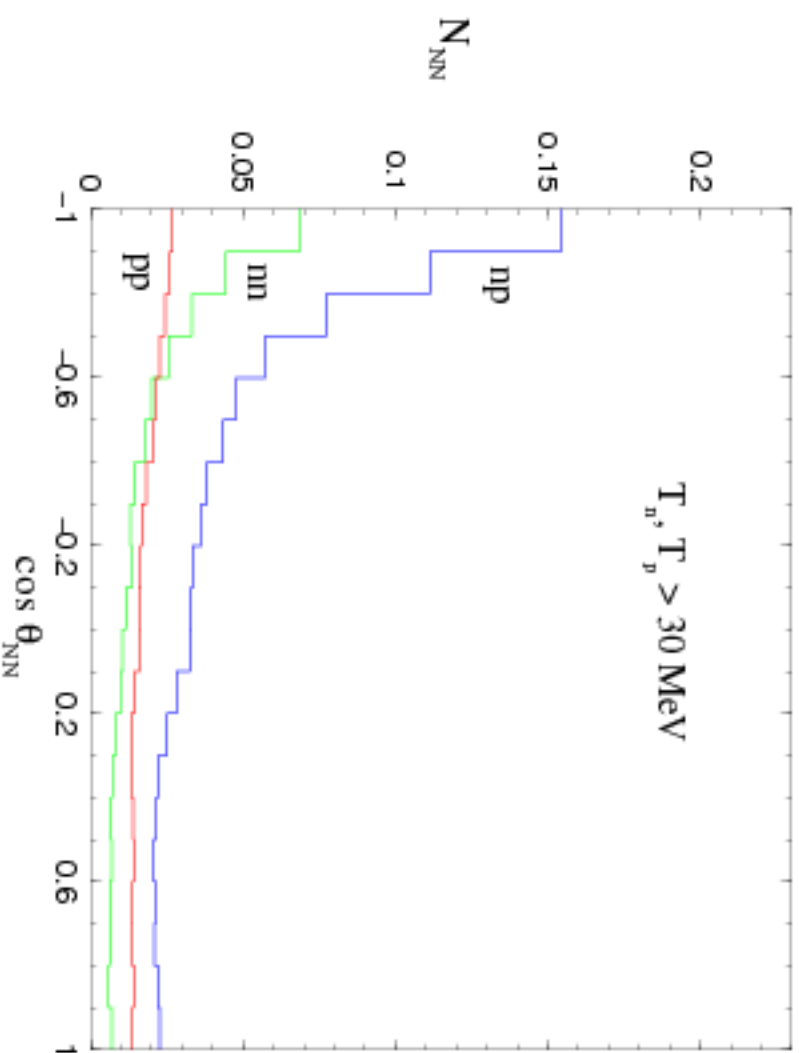
$^{12}_A\text{C} - 1\text{N}+2\text{N}$ induced

Figure 13: ANGULAR CORRELATIONS: Opening angle distributions of nm , np and pp pairs emitted per NMWD of $^{12}_A\text{C}$.

$^{12}\text{C} - 1\text{N}+2\text{N}$ induced

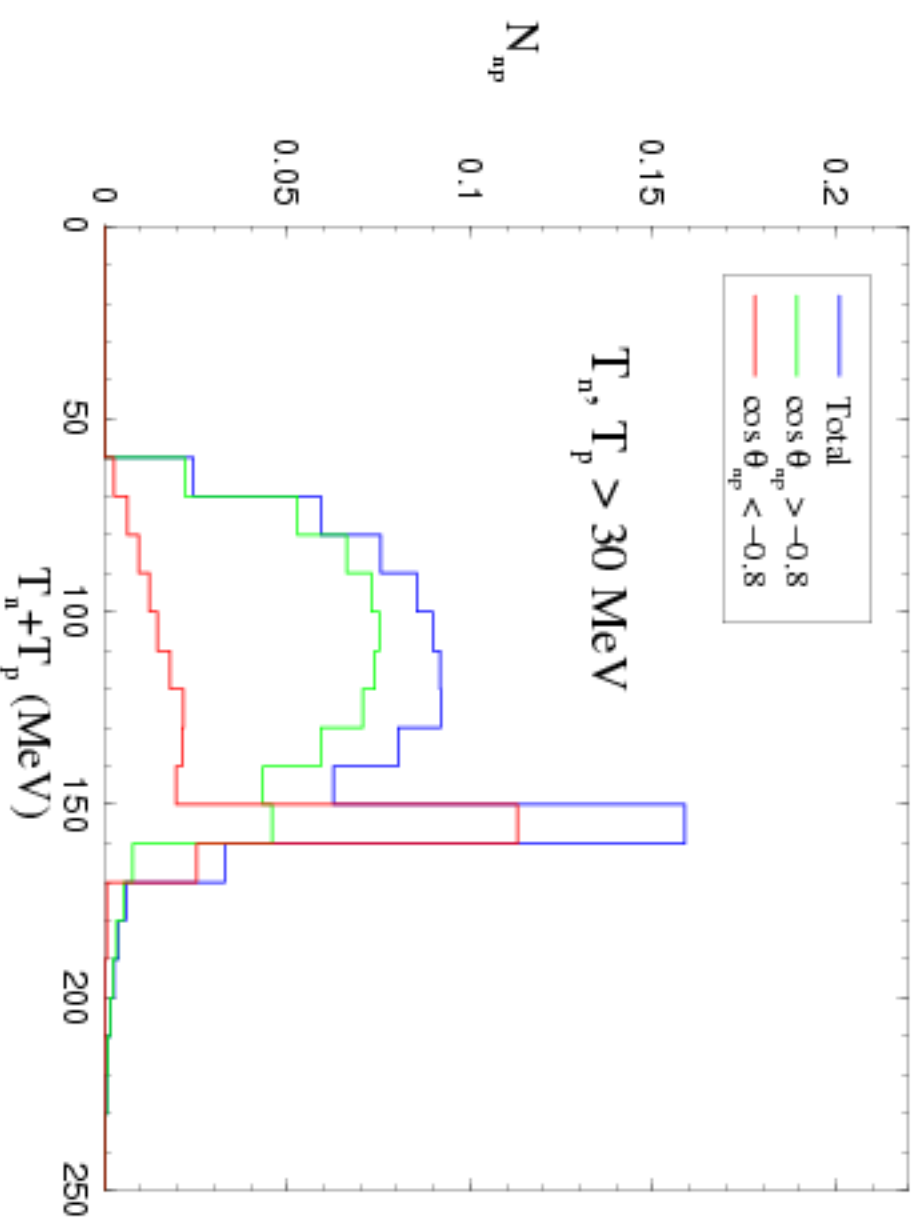


Figure 14: ENERGY CORRELATIONS of np pairs emitted per NMWD of ^{12}C .

s-shell hypernuclei and $\Delta I = 1/2$ rule

[Ref.: W.M.Alberico, G.Garbarino, PL B486 (2000) 362]

Analysis of the non-mesonic decays in *s-shell hypernuclei* allows to test the validity of the $\Delta I = 1/2$ rule.

In these hypernuclei the ΛN pair is in $L = 0$ relative state, hence only a few $\Lambda N \rightarrow NN$ transitions are allowed.

phenomenological model of Block and Dalitz

The interaction probability of a particle which crosses an infinite homogeneous system of thickness ds is $dP = ds/\lambda$, where $\lambda = 1/(\sigma\rho)$ is the mean free path.

In the process $\Lambda N \rightarrow NN$, the width $\Gamma_{NM} = dP_{\Lambda N \rightarrow NN}/dt$ is:

$$\Gamma_{NM} = v\sigma\rho$$

$v = ds/dt$ being the Λ velocity.

In nucleus of density $\rho(\vec{r})$:

$$\Gamma_{\text{NM}} = \langle v\sigma \rangle \int d\vec{r} \rho(\vec{r}) |\psi_{\Lambda}(\vec{r})|^2$$

$\langle \rangle$ is average over spin and isospin states.

Non-mesonic width $\Gamma_{\text{NM}} = \Gamma_n + \Gamma_p$ of the hypernucleus ${}_{\Lambda}^{A+1}Z$ reads:

$$\Gamma_{\text{NM}}({}_{\Lambda}^{A+1}Z) = \frac{N\bar{R}_n({}_{\Lambda}^{A+1}Z) + Z\bar{R}_p({}_{\Lambda}^{A+1}Z)}{A} \rho_{\Lambda}$$

\bar{R}_n (\bar{R}_p) being spin-averaged rate for the neutron-induced (proton-induced) process.

By introducing the rates R_{NJ} for the spin-singlet (R_{n0} , R_{p0}) and

spin-triplet (R_{n1}, R_{p1}) elementary $\Lambda N \rightarrow NN$ interactions:

$$\Gamma_{\text{NM}}({}^3_{\Lambda}\text{H}) = (3R_{n0} + R_{n1} + 3R_{p0} + R_{p1}) \frac{\rho^2}{8},$$

$$\Gamma_{\text{NM}}({}^4_{\Lambda}\text{H}) = (R_{n0} + 3R_{n1} + 2R_{p0}) \frac{\rho^3}{6},$$

$$\Gamma_{\text{NM}}({}^4_{\Lambda}\text{He}) = (2R_{n0} + R_{p0} + 3R_{p1}) \frac{\rho^3}{6},$$

$$\Gamma_{\text{NM}}({}^5_{\Lambda}\text{He}) = (R_{n0} + 3R_{n1} + R_{p0} + 3R_{p1}) \frac{\rho^4}{8}.$$

(total hypernuclear angular momentum is 0 for ${}^4_{\Lambda}\text{H}$ and ${}^4_{\Lambda}\text{He}$ and 1/2 for ${}^3_{\Lambda}\text{H}$ and ${}^5_{\Lambda}\text{He}$).

Rates associated to the partial-wave transitions:

$$R_{n0} = R_n({}^1S_0) + R_n({}^3P_0),$$

$$R_{p0} = R_p({}^1S_0) + R_p({}^3P_0),$$

$$R_{n1} = R_n({}^3P_1),$$

$$R_{p1} = R_p({}^3S_1) + R_p({}^1P_1) + R_p({}^3P_1) + R_p({}^3D_1),$$

From angular momentum coupling and assuming $\Delta I = 1/2$ it follows:

$$R_{n1}/R_{p1} \leq R_{n0}R_{p0} = 2$$

For pure $\Delta I = 3/2$ transitions, the factors 2 are replaced by 1/2 and by further introducing the ratio:

$$r = \frac{\langle I_f = 1 || A_{1/2} || I_i = 1/2 \rangle}{\langle I_f = 1 || A_{3/2} || I_i = 1/2 \rangle}$$

for a general $\Delta I = 1/2 - \Delta I = 3/2$ mixture one gets:

$$\frac{R_{n1}}{R_{p1}} = \frac{4r^2 - 4r + 1}{2r^2 + 4r + 2 + 6\lambda^2} \leq \frac{R_{n0}}{R_{p0}} = \frac{4r^2 - 4r + 1}{2r^2 + 4r + 2},$$

with:

$$\lambda = \frac{\langle I_f = 0 || A_{1/2} || I_i = 1/2 \rangle}{\langle I_f = 1 || A_{3/2} || I_i = 1/2 \rangle}$$

The partial rates supply the Γ_n/Γ_p ratios for s -shell hypernuclei. For example, for ${}^5_\Lambda\text{He}$:

$$\frac{\Gamma_n}{\Gamma_p}({}^5_\Lambda\text{He}) = \frac{R_{n0} + 3R_{n1}}{R_{p0} + 3R_{p1}}$$

NB: from these relations and experimental data it is possible to extract the spin and isospin behaviour of the $\Lambda N \rightarrow NN$ interaction without a detailed knowledge of the interaction mechanism. There are indications for a sizeable violation of $\Delta I = 1/2$ rule but more precise measurements are needed, especially for ${}^3_\Lambda\text{H}$ and ${}^4_\Lambda\text{H}$.

Experimental data and $\Delta I = 1/2$ rule

Determine the rates $R_{N,j}$ by fitting experimental data for the observables which have the smallest experimental uncertainties:

$$\Gamma_{\text{NM}}(^4\text{H}), \quad \Gamma_{\text{NM}}(^4\text{He}), \quad \Gamma_{\text{NM}}(^5\text{He}), \quad \frac{\Gamma_n}{\Gamma_p}(^4\text{He})$$

After solving previous equations for these quantities, we obtained the following partial rates (the decay widths are considered in units of the free

Λ decay width):

$$R_{n0} = (4.7 \pm 2.1) \text{ fm}^3,$$

$$R_{p0} = (7.9_{-7.9}^{+16.5}) \text{ fm}^3,$$

$$R_{n1} = (10.3 \pm 8.6) \text{ fm}^3,$$

$$R_{p1} = (9.8 \pm 5.5) \text{ fm}^3,$$

$$\bar{R}_{n({}^5_{\Lambda}\text{He})} \equiv \frac{1}{4} (R_{n0} + 3R_{n1}) = (8.9 \pm 6.5) \text{ fm}^3,$$

$$\bar{R}_{p({}^5_{\Lambda}\text{He})} \equiv \frac{1}{4} (R_{p0} + 3R_{p1}) = (9.3 \pm 5.8) \text{ fm}^3,$$

For the spin-singlet and spin-triplet ratios we have then:

$$R_{n0}/R_{p0} = 0.6_{-0.6}^{+1.3}$$

$$R_{n1}/R_{p1} = 1.0_{-1.0}^{+1.1}$$

while the ratios of the spin-triplet to the spin-singlet interaction rates are:

$$\frac{R_{n1}}{R_{n0}} = 2.2 \pm 2.1$$

$$\frac{R_{p1}}{R_{p0}} = 1.2^{+2.7}_{-1.2}$$

The large uncertainties do not allow to draw definite conclusions about the possible violation of the $\Delta I = 1/2$ rule and the spin-dependence of the transition rates. Above equations are still compatible with with the $\Delta I = 1/2$ rule.

By using the above results we can predict the neutron to proton ratio for

${}^3_\Lambda\text{H}$, ${}^4_\Lambda\text{H}$ and ${}^5_\Lambda\text{He}$, which turn out to be:

$$\frac{\Gamma_n}{\Gamma_p}({}^3_\Lambda\text{H}) = 0.7^{+1.1}_{-0.7},$$

$$\frac{\Gamma_n}{\Gamma_p}({}^4_\Lambda\text{H}) = 2.3^{+5.0}_{-2.3},$$

$$\frac{\Gamma_n}{\Gamma_p}({}^5_\Lambda\text{He}) = 0.95 \pm 0.92,$$

and, by using $\rho_2 = 0.001 \text{ fm}^{-3}$

$$\Gamma_{\text{NM}}({}^3_\Lambda\text{H}) = 0.007 \pm 0.006.$$

Non-mesonic decay of polarized Λ -hypernuclei

THE ASYMMETRY PUZZLE

Proton intensity from NMWD of Polarized Λ -hypernuclei is:

$$I(\Theta, J) = I_0(J) [1 + \mathcal{A}(\Theta, J)]$$

where:

$$I_0(J) = \frac{\text{Tr}(\mathcal{M}\mathcal{M}^\dagger)}{2J+1} = \frac{\sum_M \sigma(J, M)}{2J+1}$$

is the (isotropic) intensity for an unpolarized hypernucleus and

$$\mathcal{A}(\Theta, J) = P_y(J) \frac{3}{J+1} \frac{\text{Tr}(\mathcal{M}S_y\mathcal{M}^\dagger)(\Theta)}{\text{Tr}(\mathcal{M}\mathcal{M}^\dagger)} = P_y(J) A_y(J) \cos\Theta.$$

is the asymmetry of the angular distribution for the outgoing protons.

P_y = hypernuclear polarization

A_y = hypernuclear asymmetry parameter

$$A_y = \frac{3}{J+1} \frac{\sum_M M \sigma(J, M)}{\sum_M \sigma(J, M)}$$

In the shell model weak-coupling scheme

$$A(\Theta) = p_A a_A \cos \Theta$$

where

$$p_A = \begin{cases} -\frac{J}{J+1} P_y & \text{if } J = J_C - \frac{1}{2} \\ P_y & \text{if } J = J_C + \frac{1}{2} \end{cases}$$

Λ polarization

$$a_A = \begin{cases} -\frac{J+1}{J} A_y & \text{if } J = J_C - \frac{1}{2} \\ A_y & \text{if } J = J_C + \frac{1}{2} \end{cases}$$

intrinsic Λ asymmetry parameter

Experiments measure

$$\mathcal{A}^{\text{M}}(0^\circ) = \frac{I^{\text{M}}(0^\circ) - I^{\text{M}}(180^\circ)}{I^{\text{M}}(0^\circ) + I^{\text{M}}(180^\circ)}$$

and **determine**

$$a_{\text{N}}^{\text{M}} = \frac{\mathcal{A}^{\text{M}}(0^\circ)}{p_{\text{N}}}$$

by using an **indirect measurement** ($^5_{\text{N}}\text{He}$) or a **theoretical evaluation** ($^{12}_{\text{N}}\text{C}$) of p_{N} .

The relations

$$I^{\text{M}}(\Theta) = I_0^{\text{M}} [1 + \mathcal{A}^{\text{M}}(\Theta)]$$

$$\mathcal{A}^{\text{M}}(\Theta) = p_{\text{N}} a_{\text{N}}^{\text{M}} \cos \Theta$$

are thus assumed.

Table 4: Theory vs experiment for a_N .

| | ${}^5\text{He}$ | ${}^{12}\text{C}$ |
|-------------------------------|-----------------|-------------------|
| K. Sasaki et al. a_N | | |
| OPE | -0.44 | |
| $\pi + K$ | -0.36 | |
| $\pi + K + \text{DQ}$ | -0.68 | |
| A. Parreño et al. | | |
| OPE | -0.25 | -0.34 |
| $\pi + K$ | -0.61 | -0.64 |
| OME | -0.68 | -0.73 |
| KEK-E160 a_N^N | | -0.9 \pm 0.3 |
| KEK-E278 | 0.24 \pm 0.22 | |
| KEK-E508 (prel.) | | -0.44 \pm 0.32 |
| KEK-E462 (prel.) | 0.07 \pm 0.08 | |

Inconsistencies at the experimental level

Due to FSI, one expects $|a_N| > |a_N^M|$

RESULTS FOR THE ASYMMETRY

The calculated proton intensities are well fitted by

$$I^M(\Theta) = I_0^M [1 + p_N a_N^M \cos \Theta]$$

where

I_0^M = total number of protons emitted per NMWD

Table 5: Asymmetry parameters for ${}^5_{\Lambda}\text{He}$ and ${}^{12}_{\Lambda}\text{C}$. Preliminary data are from [T. Maruta et al., nucl-ex/0402017, HYP2003]

| | ${}^5_{\Lambda}\text{He}$ | ${}^{12}_{\Lambda}\text{C}$ |
|------------------------------------|---------------------------|-----------------------------|
| | I_0^M | I_0^M |
| | a_{Λ}^M | a_{Λ}^M |
| OPE | 0.92 | 0.93 |
| $T_N^{\text{Th}} = 0$ | 1.56 | 3.15 |
| $T_N^{\text{Th}} = 30 \text{ MeV}$ | 0.99 | 1.23 |
| $T_N^{\text{Th}} = 50 \text{ MeV}$ | 0.78 | 0.78 |
| OME | 0.69 | 0.75 |
| $T_N^{\text{Th}} = 0$ | 1.28 | 2.78 |
| $T_N^{\text{Th}} = 30 \text{ MeV}$ | 0.77 | 1.05 |
| $T_N^{\text{Th}} = 50 \text{ MeV}$ | 0.60 | 0.66 |
| KEK-E462 | 0.07 \pm 0.08 | |
| KEK-E508 | -0.44 \pm 0.32 | |